Nanoparticle-induced widening of the temperature range of liquid-crystalline blue phases

Eva Karatairi
National Centre for Scientific Research Demokritos, 15310 Aghia Paraskevi, Greece and Department of Materials Science, University of Patras, 26500 Patras, Greece

Brigita Rožič and Zdravko Kutnjak*
Condensed Matter Physics Department, Jožef Stefan Institute, Jamova cesta 39, 1000 Ljubljana, Slovenia

Vassilios Tzitzios and George Nounesis
National Centre for Scientific Research Demokritos, 15310 Aghia Paraskevi, Greece

George Cordoyiannis, Jan Thoen, and Christ Glorieux
Departement Natuurkunde en Sterrenkunde, Katholieke Universiteit Leuven, Celestijnenlaan 200D, 3001 Leuven, Belgium

Samo Kralj
Department of Physics, Faculty of Natural Sciences and Mathematics, University of Maribor, Koroška cesta 160, 2000 Maribor, Slovenia and Condensed Matter Physics Department, Jožef Stefan Institute, Jamova cesta 39, 1000 Ljubljana, Slovenia

(Received 1 December 2009; revised manuscript received 2 April 2010; published 26 April 2010)

Liquid-crystalline blue phases exhibit exceptional properties for applications in the display and sensor industry. However, in single component systems, they are stable only for very narrow temperature range between the isotropic and the chiral nematic phase, a feature that severely hinders their applicability. Systematic high-resolution calorimetric studies reveal that blue phase III is effectively stabilized in a wide temperature range by mixing surface-functionalized nanoparticles with chiral liquid crystals. This effect is present for two liquid crystals, yielding a robust method to stabilize blue phases, especially blue phase III. Theoretical arguments show that the aggregation of nanoparticles at disclination lines is responsible for the observed effects.

DOI: 10.1103/PhysRevE.81.041703 PACS number(s): 61.30.Jf, 61.30.Mp, 65.40.Ba

I. INTRODUCTION

Chiral interactions are present in a large variety of different systems [1], e.g., spin-orbit interactions in noncentrosymmetric materials, Chern-Simons interaction terms in gauge-field theories and chiral couplings in different condensed matter systems such as ferroelectrics, ferromagnets and liquid crystals (LCs). Nonlinear models, ranging from microscopic to cosmological scales, predict that they can stabilize localized states-skyrmions. Well-known examples are spin textures in quantum-Hall magnets, Turing patterns in classical liquids, skyrmions in magnetic metals, and the blue phases (BPs) in liquid crystals [2], which is the topic of this paper. In addition to fundamental physics [3,4], blue phases attract substantial interest due to their unique optical properties and potential for advanced applications, such as self-assembling tunable photonic materials and fast-light modulators [5,6]. BPs consist of a fluid lattice whose structure is stabilized by a network of topological line defects. The competition between the chiral forces and the packing topology leads to at least three different lattice structures, labeled [7] as blue phase III (BPIII), blue phase II (BPII), and blue phase I (BPI) upon decreasing the temperature from the isotropic (I) to the chiral nematic (N^*) phase. BPIII is macroscopically amorphous with a local cubic lattice in the director field, BPII is characterized by a three-dimensional cubic periodicity in the director field and BPI exhibits a body-centered cubic symmetry of the director field [7–11].

The most crucial parameters limiting the technological potential of the BPs are the high temperatures as well as the very narrow temperature range at which they appear [12]. So far, several reports exist in literature employing different strategies to widen the temperature range of BPs as well as to shift them toward the room temperature. Stabilization in a range of few K up to few tens of K has been achieved for various systems such as LC/polymers composites [13–18], LC quaternary mixtures [12] and mixtures of chiral and bent-core LCs [19]. Furthermore, a molecular design based on coupling between biaxiality and chirality as well as LC molecular geometries have been recently proposed [20,21]. Gold nanoparticles were also very recently introduced as a means of stabilizing blue phases [22].

In this paper a method of essential widening of the BPIII temperature range is presented. By means of high-resolution calorimetry we demonstrate that the temperature regime in which BPIII is stable is greatly enhanced in homogeneous mixtures of LCs and nanoparticles (NPs) of appropriate size and surface chemistry. The effect is observed for two LC compounds, one at high temperatures and one close to ambient temperature, displaying the robustness of this method. In addition, a simple model of interpreting the experimental findings is presented and the roles of the NPs type and of chirality are briefly discussed.

*Corresponding author; zdravko.kutnjak@ijs.si

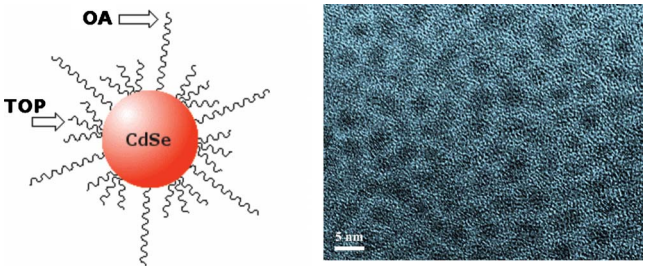

FIG. 1. (Color online) On the left, a simple schematic representation of the CdSe nanoparticles surface-treated with oleyl amine (OA) and tri-octyl phosphine (TOP) is presented. On the right a TEM image of the CdSe nanoparticles is shown.

II. SAMPLES AND EXPERIMENTAL TECHNIQUES

Two chiral LCs have been used in the present work, the S−(+)4-(2′-methylbutyl)phenyl 4′-n-octylbiphenyl-4-carboxylate (CE8 or 8SI*) and the S−(+)−4-(2-methylbutyl)phenyl 4-decyloxybenzoate (CE6). CE8 has been supplied by Merck® and CE6 by BDH®. Both compounds have been stored very carefully and used without any further treatment. They both exhibit all three BPs, as shown previously for CE6 [23] and by our present calorimetric and microscopic observations for CE8. The onset of BPIII is observed at 417.55 K for pure CE8 and at 318.43 K for pure CE6 on cooling.

For the present study, CdSe nanoparticles have been used that were surface-treated with hydrophobic oleyl amine (OA) and tri-octyl phosphine (TOP). Details on their preparation and physical characterization have been described elsewhere [24]. The so-produced CdSe NPs are essentially monodisperse and have an average diameter of 3.5 nm. They are highly soluble in nonpolar solvents such as hexane, toluene and chloroform. The morphology of the semiconducting nanoparticles as well as the nanocrystal size was investigated by transmission electron microscopy (TEM) using a CM20 Phillips® electron microscope. A simple schematic of the CdSe NPs used in this study as well as TEM image are presented in Fig. 1. Hydrophilic aerosil nanoparticles (type 300, diameter of 7 nm), purchased from Degussa, have also been used.

Mixtures of CE8 and CE6 with CdSe NPs were prepared by mixing solutions of both components in a common high-purity solvent (toluene), following the mixing procedure described elsewhere [25,26]. The resulting solution was sonicated for at least five min and then stirred for one day at 85 °C for CE8 and for three days at 65 °C for CE6, until the solvent had fully evaporated by a steady stream over the open glass vials. Thereafter, all mixtures were additionally dried under vacuum for 24 h, while slowly stirring at 75 °C for CE8 and at 55 °C for CE6 mixtures, respectively. The uniformity of the NPs distribution in the LC samples has been carefully checked using optical and fluorescence microscopy. The nanoparticle concentration, in the mixture with LCs, was defined as the mass ratio $x=m_{np}/m_{lc}$, where the index np stands for CdSe and lp for CE8 or CE6. Apart from the pure compounds, compositions of $x=0.02$, 0.07, and 0.2 have been measured for CE8 and $x=0.005$ and 0.02 for CE6, on heating and cooling.

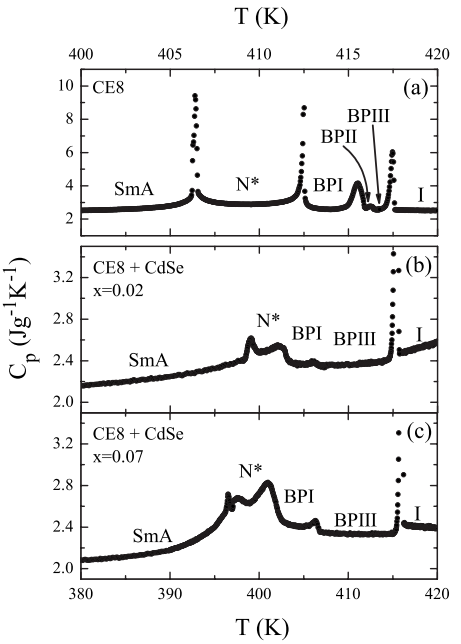

FIG. 2. Cp vs T profile for bulk CE8 (a). Temperature dependence of the ac heat capacity data for $x=0.02$ (b) and $x=0.07$ (c) mixtures of CE8+CdSe nanoparticles.

State-of-the-art calorimetric techniques have been used to obtain high-resolution data for the heat capacity temperature dependence $C_p(T)$ and derive precise phase diagrams. For CE8 the heat capacity C_p data have been obtained by ac calorimetry (ACC). Our apparatus is capable of operating in either ac or relaxation mode. The comparison of data between the two modes of operation allows for a quantitative determination of the released latent heat, when present. For CE6 the C_p profiles were obtained using adiabatic scanning calorimeter (ASC). ASC yields the temperature dependence of heat capacity and enthalpy in the same run. A detailed description of ACC and ASC, as well as their importance on revealing subtle features of phase transitions and critical phenomena in solid and soft materials, can be found elsewhere [27–31].

III. RESULTS AND DISCUSSION

The C_p data obtained by ACC for pure CE8 upon cooling the isotropic (I) to the smectic-A (SmA) phase are displayed in Fig. 2(a). Analogous runs are shown for CE8+CdSe mixtures of $x=0.02$ and 0.07 in Figs. 2(b) and 2(c), respectively. The following characteristic effects can be straightforwardly observed:

I-BPIII transition: the C_p anomaly of the I-BPIII phase transition remains sharp and analogous to the one of pure CE8 even for the highest concentration studied (i.e., $x=0.20$). The I-BPIII transition temperature remains rather close to the one of pure CE8 for all the studied mixtures. It is worth to note that even a small CdSe concentration at $x=0.02$ is enough to fully suppress the range of the BPII phase. The BPIII-BPII transition could only be observed for pure CE8, characterized by a very weak C_p peak as depicted

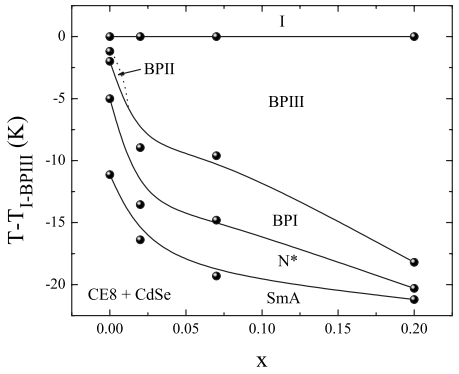

FIG. 3. T-x phase diagram for CE8+CdSe mixtures obtained in cooling runs via ACC. For clarity the data are plotted vs the $T_{I\text{–BPIII}}$ along y axis. $T_{I\text{–BPIII}}$ was found to be a weak function of x. Solid lines serve as guides to the eye.

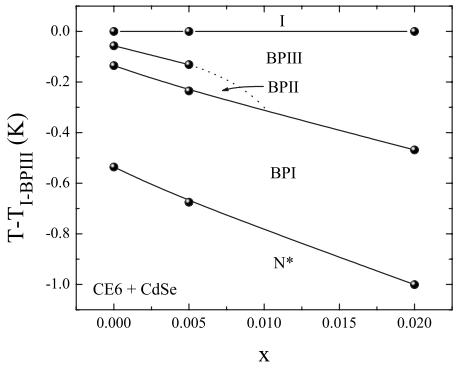

FIG. 4. T-x phase diagram for CE6+CdSe mixtures obtained in heating runs via ASC. For clarity the data are plotted vs the $T_{I\text{–BPIII}}$ along y axis. Solid lines serve as guides to the eye.

by the calorimetric profile presented in Fig. 2(a).

BPIII-BPI transition: the BPIII-BPI transition temperature is severely shifted even for the lowest studied NPs concentration and monotonously decreases with increasing x. The considerable shift to lower values of the BPIII-BPI transition combined with mild effects upon the transition temperature of the I-BPIII leads to an impressive enhancement of the phase range of BPIII. At $x=0.02$ and 0.07 the phase range is close to 10 K, while at $x=0.20$ it tends to 20 K. The phase range is not being affected by thermal hysteresis effects, remaining constant for heating and cooling runs. The temperature vs composition (T-x) phase diagram including all the phase transition lines derived by the present study, is presented in Fig. 3 for CE8. A dramatic widening of the BPIII is certainly the most striking feature of this phase diagram.

A similar effect is observed for the second compound CE6 investigated by ASC. Pure CE6 exhibits BPs much closer to the ambient temperature with respect to CE8, with BPIII appearing at a narrower range of only 57 mK [23] compared to CE8 (1.2 K). The BPIII is still present for $x=0.005$, while not for $x=0.02$, in accordance to what was observed for the respective concentration of CdSe in CE8. The BPIII range shows an significant increase by a factor of 8 times for $x=0.02$. This effect is presented in the T-x phase diagram of Fig. 4. The absolute range of BPIII remains small, but the effect on the stabilization of BPIII is equally pronounced as in the case of CE8.

In the following we discuss the two possible mechanisms behind the observed temperature widening of the BPIII phase. The first mechanism was originally proposed by Kikuchi *et al.* [14] for the polymer stabilized BPI structure. The BP structures are composed of double-twisted structure units [2] in which axes of twisting propagate in different directions. Due to topological reasons, disclination lines with the winding number $-1/2$ must be introduced. We first discuss the essential free energy terms of the simplified system in the absence of NPs, exhibiting the isotropic-blue phase-cholesteric (I-BP-N^*) phase sequence. The I-BP and BP-N^* phase transition temperatures are labeled by $T^{(I-\mathrm{BP})}$ and $T^{(\mathrm{BP}-N)}$, respectively. In the BP phase the essential free energy density contributions per disclination line distance h are given by $f \sim f_c + f_{24}$. The condensation term f_c, which is zero in the isotropic phase, strongly penalizes the presence of disclinations. We assume that the disclination cores are essentially isotropic, consequently $f_c \sim a_0(T^{(I-\mathrm{BP})}-T)S^2\pi\xi^2$. Here S stands for the equilibrium bulk orientational order parameter, a_0 is the material constant [32], and ξ is the correlation length of the orientational order parameter. The term $f_{24} \sim -\pi K_{24}$ at the interface, separating the line disclination core volume, favors the formation of blue phase structures for a positive value of the saddle-splay nematic elastic constant $K_{24} \sim k_{24}S^2$ [2], where k_{24} is temperature independent. The BP-N^* phase transition is roughly determined by the condition $f_c=-f_{24}$, yielding $T^{(\mathrm{BP}-N)} \sim T^{(I-\mathrm{BP})} - \frac{k_{24}}{a_0\xi^2}$. We assume that CdSe NPs are attracted to the disclination cores as reported in [33]. The condensation free energy penalty is decreased due to the reduced volume occupied by the energetically costly isotropic (or strongly biaxial) phase [14]. It roughly holds that $f_c \sim a_0(T^{(I-\mathrm{BP})}-T)S^2(\pi\xi^2 h - N_{\mathrm{np}}V_{\mathrm{np}})/h$ where $N_{\mathrm{np}} \propto x$ counts number of nanoparticles within h, and $V_{\mathrm{np}} \sim 4\pi R^3/3$ is the volume of the spherical particles. Consequently,

$$T^{(\mathrm{BP}-N)}(x) \sim T^{(I-\mathrm{BP})} - \frac{k_{24}}{a_0\xi^2(1-xb)}, \tag{1}$$

$b=\frac{m_{\mathrm{lc}}}{\rho_{\mathrm{np}}\xi^2 h\pi}$, where ρ_{np} stands for the mass density of nanoparticles. Therefore, the BP-N^* phase transition temperature is decreasing with increasing x, which is in agreement with the experimentally observed BP-N^* transition lines (see Fig. 3 and 4). Using Eq. (1) and requiring $T^{(\mathrm{BP}-N)}_{x=0.1} - T^{(\mathrm{BP}-N)}_{x=0} \sim 10$ K we obtain $N_{\mathrm{np}}/h \sim \xi^2/r^3 \sim 1/r$, where r is the NP radius. This rough estimate suggests that disclination lines should be almost completely saturated with NPs in order to achieve such temperature shifts. Furthermore, NPs are expected to be essentially nonuniformly distributed within disclination lines, which stabilized the amorphous BPIII-type structure with respect to more ordered BPI and BPII structures. The proposed mechanism also suggests that addition of NPs tends to increase the total disclination length within the system, because the presence of NPs strongly reduces the condensation term, while the f_{24} term is only slightly affected. Consequently, the characteristic BP lattice constant has to be reduced which is in line with recent reports [34]. Note also that

the *I*-BPIII transition line is rather weakly affected by the CdSe NPs due to the significantly larger value of ξ at $T^{(I-\mathrm{BP})}$ and, thus, the reduced disclination volume mechanism is less effective [35].

Our preliminary simulations show that the attraction force between topological defects and nanoparticles is stronger if the local ordering enforced by nanoparticles is similar to the defect core structure. In order to test this prediction, a $x=0.05$ mixture of CE8 and hydrophilic aerosil NPs was examined. The studied concentration lies in the so-called *soft network regime* [36–38], ranging in the interval $0.01<x0.10$, in which the aerosil nanoparticles form adaptive networks. Aerosils are expected to locally enforce stronger nematic ordering with respect to CdSe NPs and they tend to self-organize into a network structure. As expected, their impact on BPIII is apparently weaker. The different impact of aerosils and CdSe nanoparticles on the stability of the BPIII structure results from their different spatial distributions which is due to self-assembly tendency of aerosils and their weaker attraction to disclination lines in comparison to CdSe NPs. Consequently, the reduction in the energetically costly condensation term is less effective in aerosil-LC mixtures.

The second mechanism is related to the fact that the phase diagrams obtained for CE8 and CE6 liquid crystals, as demonstrated in Figs. 3 and 4, exhibit an analogy with the proposed generalized phase diagrams for BPs in Ref. [39]. The decrease in the lattice constant together with the above mentioned similarity of the phase diagrams indicate possible increase in the chirality with increasing the nanoparticles concentration. Namely, the surface coating chains of NPs are flexible and could adopt and even amplify the chiral tendency of LC molecules. An increase in chirality widens the BPIII phase much more than BPI phase and changes the *I*-BPIII transition temperature much less than the other transition temperatures, in agreement with our results. It should be noted that stronger compression of smectic layers was found recently in more chiral compounds indicating stronger increase in chirality in the latter [40].

IV. CONCLUSIONS

To conclude, the impact of different nanoparticles on the stability of BPs has been systematically explored for CE8 and CE6 liquid crystals, focusing on the CdSe ones that exhibit a considerable impact. In particular, it has been demonstrated that the hydrophobic surface-treated CdSe nanoparticles could greatly enhance the temperature range of the BPIII phase, approaching a range of 20 K for CE8. The reason behind this is the reduction in free energy penalties for the presence of disclination lines. This mechanism can be very effective if NPs are strongly attracted to disclination lines, which can be enforced by appropriate surface treatment of NPs and their size (it should be comparable to the characteristic core size of disclinations). On the contrary, the polymer-driven stabilization, using the same mechanism, stabilizes the BPI phase. The BPIII phase is of high technological interest because it enables among others fast electro-optical switching between dark and bright states without need for demanding specific surface treatment [41]. Hence, a and robust method for stabilizing BPIII phase is developed. This method provides a powerful tool in the hunt of photonic applications in the science and technology of liquid crystals.

ACKNOWLEDGMENTS

This work was supported by the Slovenian Research Agency (Program No. P1-0125 and Project No. J1-9368 and No. J1-2015). E.K. acknowledges the support of the N.C.S.R. "Demokritos." G.C. acknowledges the support of FWO (Project "AVISCO" nr. G.0230.07), the Research Fund of K. U. Leuven and the assistance of P. Losada-Pérez and C. S. P. Tripathi.

[1] U. K. Rößler, A. N. Bogdanov, and C. Pfleiderer, Nature (London) **442**, 797 (2006) and references therein.
[2] S. Meiboom, J. P. Sethna, P. W. Anderson, and W. F. Brinkman, Phys. Rev. Lett. **46**, 1216 (1981).
[3] Z. Kutnjak, C. W. Garland, J. L. Passmore, and P. J. Collings, Phys. Rev. Lett. **74**, 4859 (1995).
[4] M. A. Anisimov, V. A. Agayan, and P. J. Collings, Phys. Rev. E **57**, 582 (1998).
[5] W. Cao, A. Munoz, P. Palffy-Muhoray, and B. Taheri, Nat. Mater. **1**, 111 (2002).
[6] M. F. Moreira, I. C. S. Carvallo, W. Cao, C. Bailey, B. Taheri, and P. Palffy-Muhoray, Appl. Phys. Lett. **85**, 2691 (2004).
[7] P. Crooker, in *Chirality in Liquid Crystals*, edited by H.-S. Kitzerow and C. Bahr (Springer, New York, 2001).
[8] R. Barbet-Massin, P. E. Cladis, and P. Pieranski, Phys. Rev. A **30**, 1161 (1984).
[9] P. H. Keyes, Phys. Rev. Lett. **65**, 436 (1990).
[10] E. Dubois-Violette, B. Pansu, and P. Pieranski, Mol. Cryst. Liq. Cryst. **192**, 221 (1990).
[11] E. P. Koistinen and P. H. Keyes, Phys. Rev. Lett. **74**, 4460 (1995).
[12] H. J. Coles and M. N. Pivnenko, Nature (London) **436**, 997 (2005).
[13] H. S. Kitzerow, H. Schmid, A. Ranft, G. Heppke, R. A. M. Hikmet, and J. Lub, Liq. Cryst. **14**, 911 (1993).
[14] H. Kikuchi, M. Yokota, Y. Hisakado, H. Yang, and T. Kajiyama, Nat. Mater. **1**, 64 (2002).
[15] C. Bohley and T. Scharf, Proc. SPIE **5184**, 202 (2003).
[16] Y. Hisakado, H. Kikuchi, T. Nagamura, and T. Kajiyama, Adv. Mater. **17**, 96 (2005).
[17] T. Noma, M. Ojima, H. Asagi, Y. Kawahira, A. Fujii, and M. Ozaki, e-J. Surf. Sci. Nanotechnol. **6**, 17 (2008).
[18] T. Iwata, K. Suzuki, N. Amaya, H. Higuchi, H. Masunaga, S. Sasaki, and H. Kikuchi, Macromolecules **42**, 2002 (2009).
[19] M. Nakata, Y. Takanishi, J. Watanabe, and H. Takezoe, Phys. Rev. E **68**, 041710 (2003).

[20] A. Yoshizawa, H. Iwamochi, S. Segawa, and M. Sato, Liq. Cryst. **34**, 1039 (2007).
[21] A. Yoshizawa, Y. Kogawa, K. Kobayashi, Y. Takanishi, and J. Yamamoto, J. Mater. Chem. **19**, 5759 (2009).
[22] H. Yoshida, Y. Tanaka, K. Kawamoto, H. Kubo, T. Tsuda, A. Fujii, S. Kuwabata, H. Kikuchi, and M. Ozaki, Appl. Phys. Express **2**, 121501 (2009).
[23] G. Voets and W. van Dael, Liq. Cryst. **14**, 617 (1993).
[24] V. Tzitzios, V. Georgakilas, I. Zafiropoulou, N. Boukos, G. Basina, D. Niarchos, and D. Petridis, J. Nanosci. Nanotechnol. **8**, 3117 (2008).
[25] H. Haga and C. W. Garland, Phys. Rev. E **56**, 3044 (1997).
[26] Z. Kutnjak, S. Kralj, and S. Žumer, Phys. Rev. E **66**, 041702 (2002).
[27] J. Thoen, H. Marynissen, and W. Van Dael, Phys. Rev. A **26**, 2886 (1982).
[28] J. Thoen, G. Cordoyiannis, and C. Glorieux, Liq. Cryst. **36**, 669 (2009).
[29] H. Yao, K. Ema, and C. W. Garland, Rev. Sci. Instrum. **69**, 172 (1998).
[30] Z. Kutnjak, S. Kralj, G. Lahajnar, and S. Žumer, Phys. Rev. E **68**, 021705 (2003).
[31] Z. Kutnjak, J. Petzelt, and R. Blinc, Nature (London) **441**, 956 (2006).
[32] P. de Gennes and J. Prost, *The Physics of Liquid Crystals* (Oxford University Press, Oxford, 1993).
[33] D. Pires, J. B. Fleury, and Y. Galerne, Phys. Rev. Lett. **98**, 247801 (2007).
[34] M. Ravnik, G. P. Alexander, J. M. Yeomans, and Z. Žumer, Faraday Discuss. **144**, 159 (2010).
[35] Z. Kutnjak, C. W. Garland, C. G. Schatz, P. J. Collings, C. J. Booth, and J. W. Goodby, Phys. Rev. E **53**, 4955 (1996).
[36] G. S. Iannacchione, C. W. Garland, J. T. Mang, and T. P. Rieker, Phys. Rev. E **58**, 5966 (1998).
[37] J. Barré, A. R. Bishop, T. Lookman, and A. Saxena, Phys. Rev. Lett. **94**, 208701 (2005).
[38] G. Cordoyiannis, G. Nounesis, V. Bobnar, S. Kralj, and Z. Kutnjak, Phys. Rev. Lett. **94**, 027801 (2005).
[39] M. B. Bowling, P. J. Collings, C. J. Booth, and J. W. Goodby, Phys. Rev. E **48**, 4113 (1993).
[40] G. Cordoyiannis, S. Kralj, G. Nounesis, Z. Kutnjak, and S. Žumer, Phys. Rev. E **75**, 021702 (2007).
[41] M. Sato and A. Yoshizawa, Adv. Mater. **19**, 4145 (2007).